

## Structure of nuclear transition matrix elements for neutrinoless double- $\beta$ decay

P K RATH

Department of Physics, University of Lucknow, Lucknow 22 6007, India

E-mail: pkrath\_lu@yahoo.co.in

**Abstract.** The structure of nuclear transition matrix elements (NTMEs) required for the study of neutrinoless double- $\beta$  decay within light Majorana neutrino mass mechanism is disassembled in the PHFB model. The NTMEs are calculated using a set of HFB intrinsic wave functions, the reliability of which has been previously established by obtaining an overall agreement between the theoretically calculated spectroscopic properties and the available experimental data. Presently, we study the role of short-range correlations, radial evolution of NTMEs and deformation effects due to quadrupolar correlations. In addition, limits on effective light neutrino mass  $\langle m_\nu \rangle$  are extracted from the observed limits on half-lives  $T_{1/2}^{0\nu}$  of neutrinoless double- $\beta$  decay.

**Keywords.** Nuclear transition matrix elements; projected Hartree–Fock–Bogoliubov model; short-range correlations; deformation effect.

**PACS Nos** 23.40.Bw; 23.40.Hc; 21.60.Jz

### 1. Introduction

The observational data obtained from three complementary experiments, namely, single  $\beta$ -decay, neutrino oscillation and neutrinoless double beta  $(\beta\beta)_{0\nu}$  decay can ascertain the mass and nature of neutrinos. The confirmation of flavour oscillation of neutrinos in atmospheric, solar, reactor and accelerator sources has established that oscillations among three massive neutrino species are sufficient to explain the observed atmospheric and solar neutrino puzzle. Further, the neutrino oscillation experiments provide us with neutrino mass square differences  $\Delta m^2$ , mixing angles (see table 1) and three possible hierarchies, namely, normal, inverted and degenerate mass spectrum. It is generally agreed that out of the many possibilities [1–3], the observation of neutrinoless double beta  $(\beta\beta)_{0\nu}$  decay can clarify a number of issues, such as the nature of neutrinos, the origin of neutrino mass, absolute scale on neutrino mass, the possible hierarchy in the neutrino mass spectrum and CP violation in the leptonic sector.

The twelve rare experimentally distinguishable modes of nuclear  $(\beta\beta)_{0\nu}$  decay, namely the double-electron emission  $(\beta^-\beta^-)_{0\nu}$ , double-positron emission  $(\beta^+\beta^+)_{0\nu}$ , electron–positron conversion  $(\varepsilon\beta^+)_{0\nu}$  and double-electron capture  $(\varepsilon\varepsilon)_{0\nu}$  with the

**Table 1.** Global three-oscillation analysis with unconstrained  $CP$ -violating phase [4].

Parameter	Best fit	$1\sigma$ range	$2\sigma$ range	$3\sigma$ range
$\Delta m_{21}^2/10^{-5} \text{ eV}^2$	7.67	7.48–7.83	7.31–8.01	7.14–8.19
$\Delta m_{31}^2/10^{-3} \text{ eV}^2$	2.39	2.31–2.50	2.19–2.66	2.06–2.81
$\sin^2 \theta_{12}$	0.312	0.294–0.331	0.278–0.352	0.263–0.375
$\sin^2 \theta_{23}$	0.466	0.408–0.539	0.366–0.602	0.331–0.664
$\sin^2 \theta_{13}$	0.016	0.006–0.026	<0.036	<0.046

emission of no neutrinos, single Majoron and double Majorons, are semileptonic weak transitions involving strangeness conserving charged currents. The  $(\beta^+\beta^+)_{0\nu}$ ,  $(\varepsilon\beta^+)_{0\nu}$  and  $(\varepsilon\varepsilon)_{0\nu}$  modes are energetically competing and we shall refer to them as  $(e^+\beta\beta)_{0\nu}$  decay. The possible mechanisms for the occurrence of the lepton number violating  $(\beta\beta)_{0\nu}$  decay are the exchange of light as well as heavy neutrinos and the right-handed current in the left–right symmetric models (LRSM), the exchange of sleptons, neutralinos, squarks and gluinos in the  $R_p$ -violating minimal supersymmetric standard model (MSSM), the exchange of leptoquarks, existence of heavy sterile neutrinos, compositeness and extradimensional scenarios. Further, the single-Majoron-accompanied neutrinoless double beta  $(\beta\beta\phi)_{0\nu}$  decay and double-Majoron-accompanied neutrinoless double beta  $(\beta\beta\phi\phi)_{0\nu}$  decay occur in nine Majoron models [5]. The study of  $(\beta\beta)_{0\nu}$  decay can provide stringent limits on the associated gauge theoretical parameters and its observation can only judge the role of different mechanisms in various gauge theoretical models. However, the accuracy of the extracted gauge theoretical parameters depends on the reliability of nuclear transition matrix elements (NTMEs).

In the conventional nuclear structure calculations, the nucleus is treated as a non-relativistic many-body system. Further, it consists of point nucleons, which interact through two-body interactions only. The form of two-body interaction is derived from the two-nucleon data on the basis of meson exchange theory and through this procedure only the on-shell behaviour of the interaction is specified. In the perturbative approach, the non-relativistic many-body Schrödinger equation is not numerically solvable. To overcome this difficulty, the model space, effective interaction and effective operators are introduced. The effective interaction so derived can be made energy independent through Brandow’s linked cluster expansion [6] and Kuo’s folded diagram expansion [7]. Due to the limited success of the effective two-body interaction so obtained, the empirical and phenomenological effective interactions are still in use.

The nuclear models are generically mean-field models. Usually, a phenomenological mean field is used in the shell model whereas the mean field is generated in the Hartree–Fock (HF), projected Hartree–Fock–Bogoliubov (PHFB) and quasiparticle random phase approximation (QRPA) models through self-consistent procedure. However, the HF neglects the quasiparticles and their interactions, the PHFB assumes non-interacting quasiparticles and the QRPA takes care of the interaction between the quasiparticles to a certain extent. The structure of a nucleus is mainly

decided by the subtle interplay of pairing and quadrupolar correlations present in the effective two-body interaction. The shell model is the best choice to calculate the NTMEs as it attempts to solve the nuclear many-body problem as exactly as possible [8–10]. However, it is not presently possible to study the medium and heavy mass deformed nuclei in the shell model with the available computational facilities. The first explanation about the observed suppression of  $M_{2\nu}$  was given in the QRPA model [11,12]. Further, the QRPA and its extensions have emerged as the most successful models in correlating single- $\beta$  GT strengths and half-lives of  $(\beta^-\beta^-)_{2\nu}$  decay [13]. In spite of the spectacular success of the QRPA in the study of  $\beta\beta$  decay, there was a need to include the deformation degrees of freedom in its formalism and developments in this direction are in progress [14,15].

In the PHFB model, the pairing and deformation degrees of freedom are treated simultaneously and on equal footing. However, the structure of the intermediate odd  $Z$ -odd  $N$  nuclei, which provides information on the single  $\beta$ -decay rates and the distribution of GT strengths, cannot be studied in its present version of the PHFB model. In spite of this limitation, the PHFB model in conjunction with pairing plus quadrupole–quadrupole (PQQ) [16] interaction has been successfully applied to study the  $0^+ \rightarrow 0^+$  transition of  $(\beta^-\beta^-)_{2\nu}$  [17,18] and  $(e^+\beta\beta)_{2\nu}$  modes [18,19] in the mass range  $A = 90$ –150, where it was possible to describe the lowest excited states of the parent and daughter nuclei along with their electromagnetic transition strengths, as well as to reproduce the available measured  $(\beta^-\beta^-)_{2\nu}$  decay rates.

The main objective of the present work is to study the effects of short-range correlations, radial evolution of NTMEs and the effect of deformation due to quadrupolar correlations on NTMEs of  $(\beta\beta)_{0\nu}$  decay in the light Majorana neutrino mass mechanism. The required theoretical formalism has been given in detail by Doi *et al* [1,20], Haxton and Stephenson [21] as well as Tomoda [22] and the notations used in the present work can be found in refs [23–25]. In §2, the reliability of the HFB wave functions used to calculate the NTMEs for  $(\beta^-\beta^-)_{0\nu}$  decay is briefly discussed. The effects due to short-range correlations, radial evolution of NTMEs and the deformation effects are discussed in §3. In the same section, we extract limits on the effective light neutrino mass  $\langle m_\nu \rangle$  from the observed limits on the half-lives  $T_{1/2}^{0\nu}$  of  $(\beta^-\beta^-)_{0\nu}$  decay. In §4, some concluding remarks are presented.

## 2. Reliability of HFB wave functions

The HFB wave functions are generated using an effective Hamiltonian with PQQ [16] type of effective two-body interaction with two different parametrizations. Explicitly, the Hamiltonian can be written as

$$H = H_{\text{sp}} + V(\text{P}) + \zeta_{\text{QQ}}V(\text{QQ}), \quad (1)$$

where  $H_{\text{sp}}$ ,  $V(\text{P})$  and  $V(\text{QQ})$  denote the single-particle Hamiltonian, the pairing and quadrupole–quadrupole part of the effective two-body interaction, respectively. The  $\zeta_{\text{QQ}}$  is an arbitrary parameter and the purpose of introducing it is to study the role of deformation by varying the strength of the QQ interaction. The final results

are obtained by setting  $\zeta_{QQ} = 1$ . The model space, single-particle energies (SPEs) and the parameters of the pairing part of the effective two-body interactions have been given in refs [17–19].

In the case of the first parametrization, the strengths of the like particle components of the QQ interaction are taken as:  $\chi_{pp} = \chi_{nn} = 0.0105 \text{ MeV b}^{-4}$ , where  $b$  is the oscillator parameter. The strength of proton–neutron (pn) component of the QQ interaction  $\chi_{pn}$  is varied so as to obtain the spectra of the considered nuclei in the mass range  $A = 90\text{--}150$  in optimum agreement with the experimental results. The theoretical spectra are taken to be the optimum one if the excitation energy of the  $2^+$  state,  $E_{2^+}$ , is reproduced as closely as possible to the experimental value. For the second parametrization, we take  $\chi_{pp} = \chi_{nn} = \chi_{pn}/2$  and the above-mentioned procedure is adopted to fix them. We denote the first and second parametrizations as PQQ1 and PQQ2 respectively. The reliability of HFB wave functions with PQQ1 parameters has been already tested by obtaining an overall agreement between theoretically calculated yrast spectra, reduced  $B(E2:0^+ \rightarrow 2^+)$  transition probabilities, static quadrupole moments  $Q(2^+)$ ,  $g$ -factors  $g(2^+)$  and NTMEs  $M_{2\nu}$  as well as half-lives  $T_{1/2}^{2\nu}$  of  $(\beta^-\beta^-)_{2\nu}$  mode and the available experimental data [17,18]. In the case of PQQ2 parametrizations the yrast spectra,  $B(E2:0^+ \rightarrow 2^+)$ ,  $Q(2^+)$  and  $g(2^+)$  differ by about 7.5, 6 and 3%, respectively from those of PQQ1 parametrization. In table 2, we present the theoretically calculated and experimentally observed [26] deformation parameters  $\beta_2$ , which differ by about 3% for the PQQ1 and PQQ2 parametrizations. In the same table,  $M_{2\nu}$ , the NTMEs calculated in the PHFB model for the two above-mentioned parameters along with the experimentally observed average and recommended values [27] are also presented and the variation in them is about 23%.

**Table 2.** Calculated and experimental  $\beta_2$  parameters and NTMEs  $M_{2\nu}$  for the  $0^+ \rightarrow 0^+$  transition. The numbers corresponding to (a) and (b) are calculated for  $g_A = 1.25$  and 1.0 respectively. Experimental NTMEs are extracted from the recommended values of ref. [27] except for  $^{110}\text{Pd}$  [28].

	$\beta_2(\text{parent})$		$\beta_2(\text{daughter})$			$M_{2\nu}$				
	PQQ1	PQQ2	PQQ1	PQQ2	Exp. [26]	PQQ1	PQQ2	Exp. (a)	Exp. (b)	
$^{96}\text{Zr}$	0.085	0.085	0.080±0.017	0.191	0.192	0.1720±0.0016	0.058	0.055	0.047	0.073
$^{98}\text{Mo}$	0.158	0.159	0.1683±0.0028	0.205	0.204	0.1947±0.0030	0.130	0.129	–	–
$^{100}\text{Mo}$	0.231	0.230	0.2309±0.0022	0.214	0.215	0.2148±0.0011	0.104	0.105	0.122	0.191
$^{104}\text{Ru}$	0.285	0.285	0.2707±0.0020	0.216	0.216	0.209±0.007	0.068	0.064	–	–
$^{110}\text{Pd}$	0.216	0.217	0.257±0.006	0.196	0.201	0.1770±0.0039	0.133	0.126	<6.47	<10.11
$^{128}\text{Te}$	0.136	0.135	0.1363±0.0011	0.192	0.187	0.1836±0.0049	0.030	0.037	0.024	0.037
$^{130}\text{Te}$	0.117	0.117	0.1184±0.0014	0.166	0.167	0.169±0.007	0.041	0.041	0.017	0.027
$^{150}\text{Nd}$	0.276	0.276	0.2853±0.0021	0.238	0.236	0.1931±0.0021	0.033	0.032	0.032	0.050

### 3. Neutrinoless double beta decay

In the LRSM, the three possible mechanisms for  $(\beta\beta)_{0\nu}$  decay are the exchange of light neutrinos, heavy neutrinos and right-handed currents. The decay rate of  $(\beta\beta)_{0\nu}$  mode in the Majorana neutrino mass mechanism is usually calculated by taking a few approximations [1,21,22]. The non-relativistic impulse approximation is considered for the hadronic currents neglecting the recoil currents and the  $s_{1/2}$  wave states are only retained in the final leptonic states for the  $0^+ \rightarrow 0^+$  transition. The light and heavy neutrino species of mass  $m_i < 10$  MeV and  $m_i > 10$  GeV, respectively are considered. The calculation of phase space factors is made easier by not considering the finite de Broglie wavelength correction. CP conservation is assumed so that  $U_{ei}$  and  $V_{ei}$  are both real or purely imaginary depending on the CP parity of mass eigenstates of neutrinos  $N$ . Consequently, the effective light and neutrino mass  $\langle m_\nu \rangle$  and  $\langle M_N \rangle$  respectively are both real. However, Šimkovic *et al* [29] and Vergados [30] have shown that in the mass mechanism, the effects due to pseudoscalar and weak magnetism terms in the recoil current can change the NTMEs upto 30%, which remain to be investigated.

Usually, the finite nucleon size (FNS) effect is included by introducing a dipole type of form factor. The inclusion of short-range correlations (SRC) is more subtle and present investigations are directed in this direction. In a microscopic picture, the SRC arise mainly from the repulsive nucleon–nucleon potential arising due to the exchange of  $\rho$ - and  $\omega$ -mesons. The effect due to SRC has been included by Hirsch *et al* [31] through the  $\omega$ -meson exchange to study the  $(\beta^-\beta^-)_{0\nu}$  decay in heavy deformed nuclei, by Kortelainen *et al* [32] as well Šimkovic *et al* [33] in the unitary correlation operator method (UCOM) and Šimkovic *et al* [34] by self-consistent coupled cluster method (CCM). The SRC can also be incorporated phenomenologically by Jastrow-type of correlations with Miller–Spencer parametrization. By deriving the effective transition operator  $\hat{f}O\hat{f}$  for the  $(\beta^-\beta^-)_{0\nu}$  decay of  $^{48}\text{Ca}$  using Reid and Paris potentials, Wu and co-workers [35] have shown that phenomenologically determined  $f(r)$  has strong two-nucleon correlations.

Further, Šimkovic *et al* have shown that in the self-consistent CMM [34], the SRC effects of Argonne and CD-Bonn two-nucleon potentials are weak and it is possible to parametrize them by Jastrow-type of correlations within a few per cent accuracy. In the present work, the effects due to SRC are incorporated phenomenologically by Jastrow-type of correlations by the prescription

$$\langle j_1^\pi j_2^\pi J | \hat{O} | j_1^\nu j_2^\nu J' \rangle \rightarrow \langle j_1^\pi j_2^\pi J | f \hat{O} f | j_1^\nu j_2^\nu J' \rangle \quad (2)$$

using the parametrization given by Šimkovic *et al* [34]

$$f(r) = 1 - ce^{-ar^2}(1 - br^2) \quad (3)$$

with

$a = 1.1 \text{ fm}^{-2}$ ,	$b = 0.68 \text{ fm}^{-2}$ ,	$c = 1.0$ ,	Miller and Spencer,
$a = 1.59 \text{ fm}^{-2}$ ,	$b = 1.45 \text{ fm}^{-2}$ ,	$c = 0.92$ ,	Argonne <i>NN</i> potential,
$a = 1.52 \text{ fm}^{-2}$ ,	$b = 1.88 \text{ fm}^{-2}$ ,	$c = 0.46$ ,	CD-Bonn <i>NN</i> potential.

**Table 3.** NTMEs  $M_{0\nu}$  calculated in the PHFB model with Jastrow-type SRC for Miller–Spencer, Argonne and CD-Bonn parametrizations.

Nuclei	PQQ1				PQQ2			
	F	F+S			F	F+S		
		SRC1	SRC2	SRC3		SRC1	SRC2	SRC3
$^{96}\text{Zr}$	1.6914	1.4534	1.6795	1.7461	1.6168	1.3878	1.6051	1.6692
$^{98}\text{Mo}$	3.8253	3.3661	3.8149	3.9442	3.8453	3.3815	3.8347	3.9654
$^{100}\text{Mo}$	3.7206	3.2518	3.7141	3.8460	3.7486	3.2767	3.7419	3.8746
$^{104}\text{Ru}$	2.7004	2.3471	2.6995	2.7987	2.5395	2.2068	2.5389	2.6324
$^{110}\text{Pd}$	4.3960	3.8491	4.3891	4.5426	4.2164	3.6922	4.2094	4.3564
$^{128}\text{Te}$	1.8708	1.6249	1.8629	1.9319	2.2260	1.9446	2.2187	2.2978
$^{130}\text{Te}$	2.5088	2.2160	2.5051	2.5877	2.4698	2.1805	2.4660	2.5475
$^{150}\text{Nd}$	1.8178	1.6158	1.8187	1.8757	1.7763	1.5787	1.7773	1.8330

**Table 4.** Limits on the effective light neutrino mass  $\langle m_\nu \rangle$  from the observed limits on half-lives  $T_{1/2}^{0\nu}$  of  $(\beta^-\beta^-)_{0\nu}$  decay.

Nuclei	$T_{1/2}^{0\nu}(\text{Exp.})$	Ref.	$\langle m_\nu \rangle$					
			PQQ1			PQQ2		
			SRC1	SRC2	SRC3	SRC1	SRC2	SRC3
$^{96}\text{Zr}$	$9.2 \times 10^{21}$	[36]	15.05	13.03	12.53	15.76	13.63	13.11
$^{98}\text{Mo}$	$1.0 \times 10^{14}$	[37]	$3.60 \times 10^6$	$3.18 \times 10^6$	$3.07 \times 10^6$	$3.59 \times 10^6$	$3.16 \times 10^6$	$3.06 \times 10^6$
$^{100}\text{Mo}$	$4.6 \times 10^{23}$	[38]	1.08	0.94	0.91	1.07	0.93	0.90
$^{110}\text{Pd}$	$6.0 \times 10^{17}$	[28]	$1.44 \times 10^3$	$1.26 \times 10^3$	$1.22 \times 10^3$	$1.50 \times 10^3$	$1.31 \times 10^3$	$1.27 \times 10^3$
$^{128}\text{Te}$	$1.1 \times 10^{23}$	[39]	22.05	19.23	18.54	18.42	16.15	15.59
$^{130}\text{Te}$	$3.0 \times 10^{24}$	[40]	0.63	0.56	0.54	0.64	0.56	0.55
$^{150}\text{Nd}$	$1.2 \times 10^{21}$	[41]	19.85	17.63	17.10	20.31	18.04	17.50

In table 3, we present the NTMEs  $M_{0\nu}$  calculated in the PHFB model due to PQQ1 and PQQ2 parametrizations including standard FNS correction and Jastrow-type of SRC with Miller and Spencer, Argonne and CD-Bonn parametrizations. We denote them as SRC1, SRC2 and SRC3 for convenience. It is interesting to note that the NTMEs due to both PQQ1 and PQQ2 parametrizations are quite close. In our earlier work [23], we have shown that the NTMEs change by 17–22% due to FNS for PQQ1 parameters. The NTMEs further change by about 15%, less than 1% and less than 3.5% due to SRC1, SRC2 and SRC3, respectively. We tabulate the extracted limits on  $\langle m_\nu \rangle$  from the observed half-lives,  $T_{1/2}^{0\nu}$ , of  $(\beta^-\beta^-)_{0\nu}$  decay in table 4. The most stringent limit on  $\langle m_\nu \rangle$  is obtained for the  $^{130}\text{Te}$  nucleus.

Structure of nuclear transition matrix elements

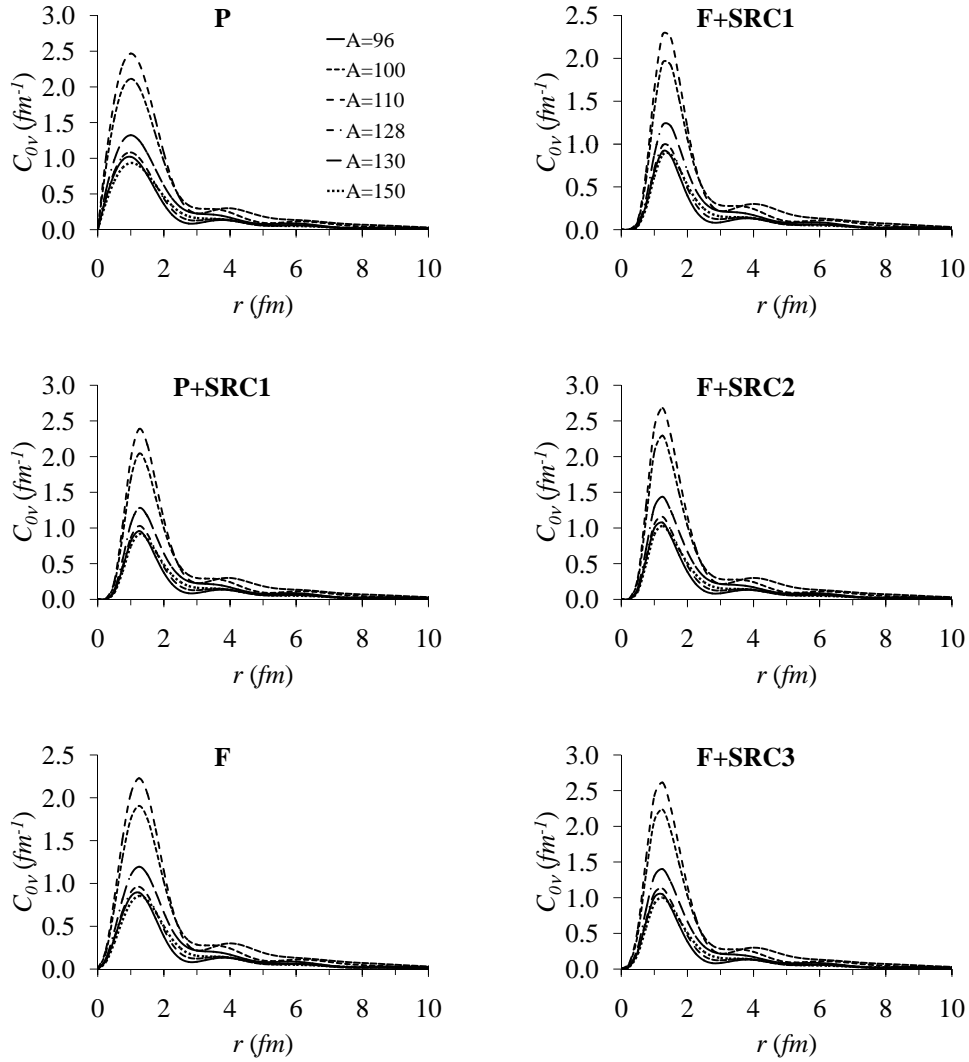


**Figure 1.** Radial distribution of NTMEs with Jastrow-type SRC for Miller–Spencer, Argonne and CD-Bonn parametrizations.

3.1 Radial evolution of NTMEs

The radial dependence of  $C_{0\nu}(r)$  defined by

$$M_{0\nu} = \int C_{0\nu}(r) dr \quad (4)$$

has been studied in the QRPA by Šimković *et al* [33] and in ISM by Menéndez *et al* [10]. In both QRPA and ISM calculations, it has been established that the

**Table 5.** Deformation ratio  $D_\alpha$  for  $^{96}\text{Zr}$ ,  $^{98}\text{Mo}$ ,  $^{100}\text{Mo}$ ,  $^{104}\text{Ru}$ ,  $^{110}\text{Pd}$ ,  $^{128}\text{Te}$ ,  $^{130}\text{Te}$  and  $^{150}\text{Nd}$  isotopes.

Ratio		$^{96}\text{Zr}$	$^{98}\text{Mo}$	$^{100}\text{Mo}$	$^{104}\text{Ru}$	$^{110}\text{Pd}$	$^{128}\text{Te}$	$^{130}\text{Te}$	$^{150}\text{Nd}$
$D_{2\nu}$		3.67	1.86	2.34	5.49	3.15	4.73	3.00	5.94
$D_{0\nu}$	P	4.31	1.93	2.11	3.66	2.56	4.25	2.93	6.18
	P+SRC1	4.47	1.94	2.14	3.78	2.62	4.40	2.95	6.17
	P+SRC2	4.37	1.94	2.12	3.69	2.58	4.31	2.94	6.18
	P+SRC3	4.32	1.93	2.11	3.66	2.56	4.31	2.93	6.18
	F	4.39	1.94	2.13	3.73	2.59	4.33	2.94	6.17
	F+SRC1	4.50	1.94	2.15	3.81	2.64	4.43	2.96	6.16
	F+SRC2	4.41	1.94	2.13	3.73	2.60	4.35	2.95	6.17
	F+SRC3	4.39	1.94	2.13	3.72	2.59	4.35	2.94	6.17

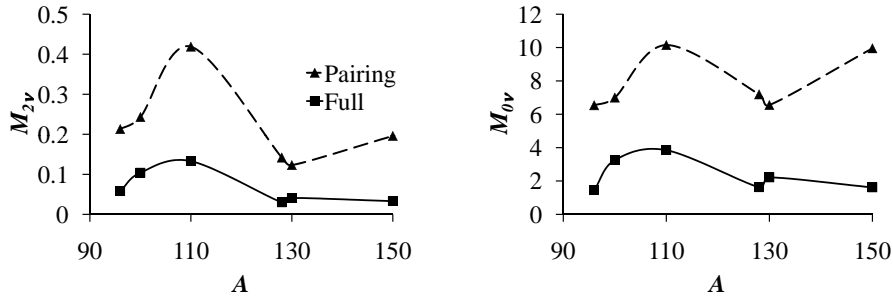


**Figure 2.** A-dependence of NTMEs  $M_{2\nu}$  and  $M_{0\nu}$  for  $\beta^-\beta^-$  decay modes.

contributions of decaying pairs coupled to  $J = 0$  and  $J > 0$  almost cancel beyond  $r \approx 3$  fm and the magnitude of  $C_{0\nu}(r)$  for all nuclei undergoing  $(\beta^-\beta^-)_{0\nu}$  decay are the maximum about the internucleon distance  $r \approx 1$  fm.

In figure 1, we plot the radial dependence of  $C_{0\nu}(r)$  for point nucleons (P) and finite-size nucleons (F) with and without Jastrow-types of SRC, which are peaked at  $\approx 1.0$  fm in the case of point nucleons and  $\approx 1.2$  fm for all other cases. It is further noticed that the radial distribution is almost negligible beyond  $r \approx 3$  fm. In addition, a weak dependence of NTMEs  $M_{0\nu}$  on Argonne and CD-Bonn parametrizations for Jastrow-type of SRC can also be noticed. Hence, it is quite necessary to include the SRC properly in the calculation of reliable NTMEs.

### 3.2 Deformation effects

The multipolar correlations in general and the quadrupolar correlations in particular are responsible for the deformation of nuclei. The role of deformation on NTMEs  $M_{2\nu}$  and  $M_\alpha$  ( $\alpha = F, GT, Fh, GTh$ ) of  $\beta^-\beta^-$  decay modes has been studied by investigating the variation of the latter by changing the strength of the QQ interaction  $\zeta_{\text{qq}}$  [17,18,23]. It was noticed that the NTMEs are usually large for  $\zeta_{\text{qq}} = 0.0$ , i.e., when both the parent and daughter nuclei are spherical. With



the increase of  $\zeta_{\text{QQ}}$ , the NTMEs remain almost constant and then decrease around the physical value  $\zeta_{\text{QQ}} = 1.0$  establishing an inverse correlation between  $M_{2\nu}$ ,  $M_F$ ,  $M_{GT}$ ,  $M_{Fh}$  as well as  $M_{GT_h}$  and  $\beta_2$ . Further, the effect of deformation on  $M_\alpha$  can be quantified by defining a quantity  $D_\alpha = M_\alpha(\zeta_{\text{QQ}} = 0)/M_\alpha(\zeta_{\text{QQ}} = 1)$ . The ratios  $D_\alpha$  reflect the suppression of the NTMEs for  $\beta\beta$ -decay with respect to the spherical case. The tabulated ratios  $D_{2\nu}$  and  $D_{0\nu}$  for point nucleons (P), point plus SRC (P+SRC), FNS (F) and FNS plus SRC (F+SRC) given in table 5 suggest that the NTMEs  $M_{2\nu}$  and  $M_{0\nu}$  are suppressed by factors of 2–6 in the mass range  $A = 90$ –150 due to deformation effects. Further, the deformation ratios  $D_{2\nu}$  and  $D_{0\nu}$  change almost equally. Hence, it is clear that the deformation effects are important in the case of  $(\beta\beta)_{0\nu}$  modes as well as  $(\beta\beta)_{2\nu}$  modes so far as the nuclear structure aspect of nuclear  $\beta\beta$ -decay is concerned.

The  $A$  dependence of  $|M_{2\nu}|$  and  $|M_{0\nu}|$  for  $\beta^-\beta^-$  modes presented in the left and right panel of figure 2, respectively, with and without quadrupolar correlations exhibit again that in the absence of quadrupolar correlations, the NTMEs are large and are suppressed with the inclusion of quadrupolar correlations in proportion to the difference in deformations between the parent and daughter nuclei. In addition, a dependence on the shell structure is observed.

#### 4. Conclusions

In the present work, we study the effects of Jastrow-type SRC with Miller–Spencer, Argonne and CD-Bonn parametrizations. It is observed that the effects of the latter two parametrizations are weak in comparison to the usual Miller–Spencer parametrization. Further, the study of radial evolution of NTME of the  $(\beta^-\beta^-)_{0\nu}$  mode for  $^{96}\text{Zr}$ ,  $^{100}\text{Mo}$ ,  $^{110}\text{Pd}$ ,  $^{128}\text{Te}$ ,  $^{130}\text{Te}$  and  $^{150}\text{Nd}$  isotopes with the three above-mentioned SRC confirm the earlier observations made in ISM and QRPA that the radial distributions of NTMEs are peaked around the internucleon separation and the maximum contributions are within 3 fm.

The PHFB model with the PQQ interaction is a convenient choice to study the role of quadrupolar correlations *vis-à-vis* deformation on NTMEs for  $\beta\beta$  decay. In our earlier work [17,18,23,25], the existence of an inverse correlation between the quadrupole deformation and the size of NTMEs  $M_{2\nu}$  and  $M_{0\nu}$  has been confirmed. In addition, it has been observed that the NTMEs are usually large in the absence of quadrupolar correlations. With the inclusion of the quadrupolar correlations, the NTMEs are almost constant for small admixture of the QQ interaction and suppressed substantially in realistic situation. In the mass range  $A = 90$ –150, the suppression factor  $D_\alpha$  between the  $\beta^-\beta^-$  decay NTMEs evaluated without and with the quadrupole–quadrupole interaction ranges between two and six, both for the  $2\nu$  and  $0\nu$  decay modes. In addition, it is also found that the NTMEs for  $\beta\beta$  decay have a well-defined maximum when the deformation of parent and daughter nuclei are similar and they are suppressed for a difference in the deformation [23–25]. To conclude, the independent deformations of initial and final nuclei are important parameters to describe the NTMEs  $M_{2\nu}$  and  $M_{0\nu}$  for  $\beta^-\beta^-$  decay modes.

## Acknowledgements

The author thanks his collaborators Drs J G Hirsch, UNAM, Mexico, P K Raina, R Chandra, IIT, Kharagpur and K Chaturvedi, Bundelkhand University, India for valuable scientific discussions. This work has been partially supported by DST, India vide sanction No. SR/S2/HEP-13/2006.

## References

- [1] M Doi, T Kotani and E Takasugi, *Prog. Theor. Phys. Suppl.* **83**, 1 (1985)
- [2] J D Vergados, *Phys. Rep.* **133**, 1 (1986)
- [3] R N Mohapatra and P B Pal, *Massive neutrinos in physics and astrophysics* (World Scientific, Singapore, 2004)
- [4] G L Fogli *et al*, *Phys. Rev.* **D78**, 033010 (2008)
- [5] P Bamert, C P Burgess and R N Mohapatra, *Nucl. Phys.* **B449**, 25 (1995)
- [6] B H Brandow, *Rev. Mod. Phys.* **39**, 771 (1967)
- [7] T T S Kuo, *Lecture notes in physics* edited by T T S Kuo and S S M Wong (Springer, Berlin, 1981) Vol. 144, p. 248
- [8] E Caurier, J Menéndez, F Nowacki and A Poves, *Phys. Rev. Lett.* **100**, 052503 (2008)
- [9] E Caurier, F Nowacki and A Poves, *Eur. Phys. J.* **A36**, 195 (2008)
- [10] J Menéndez, A Poves, E Caurier and F Nowacki, *Nucl. Phys.* **A818**, 139 (2009); arXiv:0809.2183v1[nucl-th].
- [11] P Vogel and M R Zirnbauer, *Phys. Rev. Lett.* **57**, 3148 (1986)
- [12] O Civitarese, A Faessler and T Tomoda, *Phys. Lett.* **B196**, 11 (1987)
- [13] J Suhonen and O Civitarese, *Phys. Rep.* **300**, 123 (1998)
- [14] F Šimkovic, L Paceaescu and A Faessler, *Nucl. Phys.* **A733**, 321 (2004)
- [15] M S Yousef, V Rodin, A Faessler and F Šimkovic, *Phys. Rev.* **C79**, 014314 (2009)
- [16] M Baranger and K Kumar, *Nucl. Phys.* **A110**, 490 (1968)
- [17] R Chandra, J Singh, P K Rath, P K Raina and J G Hirsch, *Eur. Phys. J.* **A23**, 223 (2005)
- [18] S Singh, R Chandra, P K Rath, P K Raina and J G Hirsch, *Eur. Phys. J.* **A33**, 375 (2007)
- [19] P K Raina, A Shukla, S Singh, P K Rath and J G Hirsch, *Eur. Phys. J.* **A28**, 27 (2006)
- [20] M Doi and T Kotani, *Prog. Theor. Phys.* **87**, 1207 (1992); **89**, 139 (1993)
- [21] W C Haxton and G J Stephenson Jr., *Prog. Part. Nucl. Phys.* **12**, 409 (1984)
- [22] T Tomoda, *Rep. Prog. Phys.* **54**, 53 (1991)
- [23] K Chaturvedi, R Chandra, P K Rath, P K Raina and J G Hirsch, *Phys. Rev.* **C78**, 054302 (2008)
- [24] P K Rath, R Chandra, K Chaturvedi, P K Raina and J G Hirsch, *Phys. Rev.* **C80**, 044303 (2009)
- [25] R Chandra, K Chaturvedi, P K Rath, P K Raina and J G Hirsch, *Europhys. Lett.* **86**, 32001 (2009)
- [26] S Raman, C W Nestor Jr and P Tikkanen, *At. Data Nucl. Data Tables* **78**, 1 (2001)
- [27] A S Barabash, arXiv:0908.4173v1 [nucl-ex]
- [28] R G Winter, *Phys. Rev.* **85**, 687 (1952)
- [29] F Šimkovic, G Pantis, J D Vergados and A Faessler, *Phys. Rev.* **C60**, 055502 (1999)
- [30] J D Vergados, *Phys. Rep.* **361**, 1 (2002)

*Structure of nuclear transition matrix elements*

- [31] J G Hirsch, O Castaños and P O Hess, *Nucl. Phys.* **A582**, 124 (1995)
- [32] M Kortelainen and J Suhonen, *Phys. Rev.* **C76**, 024315 (2007)  
M Kortelainen, O Civitarese, J Suhonen and J Toivanen, *Phys. Lett.* **B647**, 128 (2007)
- [33] F Šimkovic, A Faessler, V Rodin, P Vogel and J Engel, *Phys. Rev.* **C77**, 045503 (2008)
- [34] F Šimkovic, A Faessler, H Muether, V Rodin and M Stauf, arXiv:0902.0331v1 [nucl-th].
- [35] H F Wu, H Q Song, T T S Kuo, W K Cheng and D Strottman, *Phys. Lett.* **B162**, 227 (1985)
- [36] J Argyriades *et al*, arXiv:0906.2694v2 [nucl-ex].
- [37] J H Fremlin and M C Walters, *Proc. Phys. Soc. London* **A65**, 911 (1952)
- [38] R Arnold *et al*, *Phys. Rev. Lett.* **95**, 182302 (2005)
- [39] C Arnaboldi *et al*, *Phys. Lett.* **B557**, 167 (2003)
- [40] C Arnaboldi *et al*, *Phys. Rev.* **C78**, 035502 (2008)
- [41] A De Silva, M K Moe, M A Nelson and M A Vient, *Phys. Rev.* **C56**, 2451 (1997)